WATER DROP SIZE NUMERICAL OPTIMIZATION FOR HYDROSOLAR ROOF

Lucas M., Martínez P., Kaiser A. S., Viedma A., Zamora B.
Dpto. Ing. Térmica y de Fluidos. Universidad Politécnica de Cartagena

Campus Muralla del Mar C/ Dr Fleming, s/n

e-mail: manuel.lucas@upct.es

Abstract

Air-conditioning systems of buildings and other industrial facilities commonly use water as a heat drain to remove heat from refrigerant condensers. Classical solutions to reduce the temperature of this service water are air cooled heat exchangers or mechanical draught cooling towers. The Hydrosolar Roof optimized in this paper, working as a heat focus in the thermodynamic cycle of a heat pump, achieves the same objectives without fan energy consumption. This system consists of an extended framework on the roof of the building with some thermal plates installed over it. Some of the plates are made of a high reflective material, and the others are made of absorbent material. The Hydrosolar Roof uses the design of the reflective and absorbent parts of the device, made of flat plates, to form a sloping channel. Solar radiation is collected by this channel and, due to local heating in this zone, natural convection through it is produced. The natural induced air flow is irrigated with water sprays, placed below the plates at the inlet of the channel, generating a cross flow between air and water. In this way, water is cooled by direct contact with a reduced amount of vaporization, and most of the water is recovered at a reduced temperature. This work shows the numerical study to obtain an optimum for the sprayed water drop size. The two-dimensional version of the CFD code Fluent was applied to predict both atmospheric air and sprayed water main variables in a real geometry and under different thermodynamic conditions.

(Keywords: Drop size, Air-conditioning, solar chimney, cooling tower, solar energy)

1. Introduction

Air-conditioning systems of buildings and other industrial facilities commonly use water as a heat drain to remove heat from refrigerant condensers. Classical solutions to reduce the temperature of this service water usually are mechanical draught cooling towers. A cooling tower cools water by a combination of heat and mass transfer. In this kind of installations fans circulate atmospheric air. The water to be cooled is distributed in the tower to expose a large water surface area to atmospheric air owing to the fact that this contact area defines heat and mass exchange. A portion of the water absorbs heat to change from liquid to vapor at constant pressure. This heat of vaporization at atmospheric pressure is transferred from the water remaining in the liquid state into the airstream.

Fundamentals of this physical phenomena were described by Merkel (1925) and after by Nottage (1941). Others authors, like Mohiuddin and Kant (1996) have contributed with studies about the cooling tower systematic design. Benton and Waldrop (1988) developed a numerical simulation of transport phenomena in evaporative cooling towers with a model that later compared with experimental data. Milosavljevic and Heikkila (2001) simulated the flow in cooling towers with CFD software, reflecting both convective and heat and mass transfer effects.

Many mechanical draught cooling tower designs are now on the market and all these use conventional energy to trigger the fans and produce the air flow. The prototype showed in this paper works in the same way, however it uses renewable energy, like solar and wind energy, to achieve the same objective. Taking into account the energy demand increasing, the Hydrosolar Roof represents a clear alternative to air-conditioning and other industrial facilities heat dissipation.

Several authors have studied this particular cooling tower. Kaiser and Viedma (2001) developed an experimental study of the first generation Hydrosolar Roof and showed its

energy performance. Kaiser et al. (2001) (a) optimized the system heat dissipation and changed the Hydrosolar Roof design according to different parameters suchas air mass flow and solar radiation, among others. Zamora et al. (2000) simulated the natural convection heat transfer in the solar chimney with Fluent, a CFD code, and they compared the numerical results with the experimental results. Kaiser et al. (2001) (b) numerically established the exhauster installation influence on the chimney outlet and the natural and forced air mass flow induced. Kaiser et al. (2002) simulated direct contact heat and mass transfer with the second generation Hydrosolar Roof using Fluent and they compared the numerical results with the experimental results obtained previously

After design optimisation, by using this paper, the work to obtain the optimal working conditions began. This paper shows the numerical study to obtain an optimum for the sprayed water drop size. On one hand, reducing water drop size it is possible to increase the air and water contact surface area and therefore, improving heat dissipation. However, on the other hand, it is necessary to increase water pumping pressure, and more energy is employed to reduce water drop size. To find the optimum water drop size, a two-dimensional version of the CFD code Fluent was applied. This was to predict both atmospheric air and sprayed water variables in a real geometry and under different thermodynamic conditions.

2. System Description

The Hydrosolar Roof is mounted on the roof of the buildings and is made of a metallic structure and an hydraulic circuit. The structure is composed of a framework made of steel, which gives support to both the set solar collector and the hydraulic subsystem. The interior space allows air to move across it from bottom to top without obstacles, but it can be considered divided into two different zones from a functional point of view. The upper part, known as convection zone, is made up of sloping channels whose walls are solar collector panels. The solar radiation impinges on these panels increasing their temperature above the environmental temperature. The air located inside the channels is heated by means of convection and the natural draft produces an upward air flow. Therefore, the upper zone basically is a solar chimney. The lower part, known as the evaporative cooling zone, has a series of nozzles that spray water crosscurrent the upward air flow. The water exchanges mass and energy with the air flow and is recovered colder. This zone works as a counter flow cooling tower. The whole system can be regarded as a two-dimensional solar chimney coupled to a widespread cooling tower.

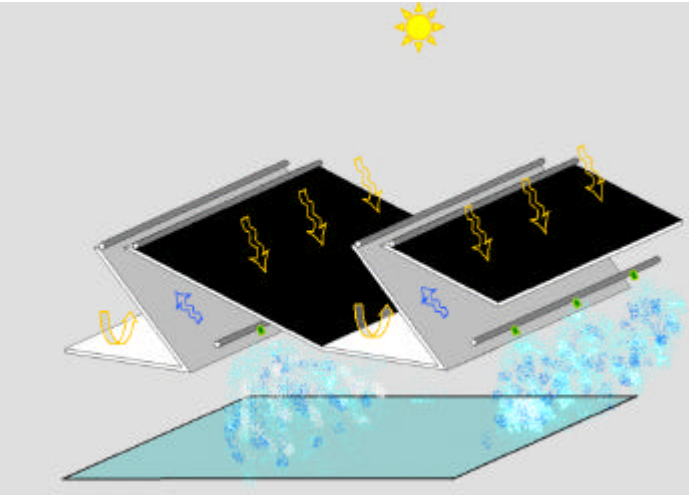

Figure 1: Hydrosolar Roof Sketch

3. Mathematical Model

Processes related to fluid fluxes and heat and mass transfer between different phases are governed by mass, momentum, energy and species conservation principia. These principia may be expressed by means of differential equations. In order to analyse the mathematical model of the problem that has been treated here, three groups of equations may be considered: the group of equations that govern the continuous phase (mass flow in the chimney produced by natural convection), the group of equations of the discrete phase (drops of water that has been sprayed), and the group of equations that provide the chemical species (dry air and water vapour). The continuous and discrete phase equations are coupled by the source terms of conservation equations. The equations of the continuous phase are represented below.

$$\frac{\partial \rho}{\partial t} + \frac{\partial}{\partial x_i}(\rho v_i) = S_{i'}, \tag{1}$$

$$\rho \frac{\mathrm{d}v_i}{\mathrm{d}t} = \frac{\partial}{\partial x_j}\left[\mu\left(\frac{\partial v_i}{\partial x_j} + \frac{\partial v_j}{\partial x_i}\right) - \frac{2}{3}\mu\left(\frac{\partial v_j}{\partial x_j}\right)\delta_{ij}\right] + \rho f_{mi} - \frac{\partial P}{\partial x_i} + F_i, \tag{2}$$

$$\rho\left(\frac{\partial e}{\partial t} + v_i \frac{\partial e}{\partial x_i}\right) = -p\frac{\partial v_i}{\partial x_i} + \Phi_v + \frac{\partial}{\partial x_i}\left(k\frac{\partial T}{\partial x_i}\right) + \frac{\partial}{\partial x_i}\left(\sum_{j=1}^{n} h_{j'} J_{j'}\right) + S_h, \tag{3}$$

$$\rho\left(\frac{\partial m_{i'}}{\partial t} + v_i \frac{\partial m_{i'}}{\partial x_i}\right) = -\frac{\partial J_{i',i}}{\partial x_i} + S_{i'}, \tag{4}$$

$$J_{i',i} = -\rho D_{i',m}\frac{\partial m_{i'}}{\partial x_i}, \tag{5}$$

where $S_{i'}$, F_i y S_h represent the source terms, $m_{i'}$ is the local mass fraction of the specie i', $\sum_{j=1}^{n} h_{j'} J_{j'}$ is enthalpy transport due to diffusion of specie j', $J_{i',i}$ is the diffusion flux of specie i', and $D_{i',m}$ is the diffusion coefficient of specie i' in the mixture.

The trajectory of a discrete phase particle (droplet) may be predicted by integrating the force balance on the particle, which is written in a Lagrangian reference frame. This force balance equates the particle inertia with the forces acting on the particle, and can be written (for the x direction in Cartesian coordinates) as equation (6). On the other hand, energy balance for the particle is also considered in equation (8).

$$\frac{\mathrm{d}u_{p_i}}{\mathrm{d}t} = \frac{18\mu}{\rho_p D_p^2}\frac{C_D \mathrm{Re}}{\partial x_i}\left(v_i - u_{p_i}\right) + g_i\frac{\left(\rho_p - \rho\right)}{\rho_p} + \frac{\rho}{\rho_p}u_{p_i}\frac{\partial v_i}{\partial x_i}, \tag{6}$$

$$\frac{\mathrm{d}x_i}{\mathrm{d}t} = u_p \tag{7}$$

$$m_p C_p \frac{\mathrm{d}T_p}{\mathrm{d}t} = hA_p\left(T_\infty - T_p\right) + \frac{\mathrm{d}m_p}{\mathrm{d}t}h_{f_g}, \tag{8}$$

$$\mathrm{Re} = \frac{\rho D_p\left(u_{p_i} - v_i\right)}{\mu}, \tag{9}$$

$$C_D = a_1 + \frac{a_2}{\mathrm{Re}} + \frac{a_3}{\mathrm{Re}^2}, \tag{10}$$

$$F_D = \frac{18\mu}{\rho_p D_p^2}\frac{C_D \mathrm{Re}}{\partial x_i}, \tag{11}$$

where a_i ´s coefficients are constants that apply for smooth spherical particles over several ranges of Re given by Morsi and Alexander (1972), $F_D(v_i - u_{pi})$ is the drag force per unit particle mass, $g_i(\rho_p - \rho)/\rho_p$ is the gravity force per unit particle mass, and $(\rho/\rho_p)u_{pi}(\partial v_i/\partial x_i)$ is the force due to the pressure gradient in the fluid, where v_i and ρ are the velocity and density in the continuous phase; u_{pi}, ρ_p, m_p, T_p, h_{fg} y C_p the velocity, density, mass, temperature, latent heat, heat capacity of the particle, h the convection heat transfer coefficient and $\mathrm{d}m_p/\mathrm{d}t$ the

rate of evaporation in the particle.

The process of coupling between discrete and continuous phase are solved by an iterative method. As the trajectory of a particle is computed, the code keeps track of the heat, mass, and momentum gained or lost by the particle stream that follows that trajectory and these quantities can be incorporated in the subsequent continuous phase calculations. Thus, while the continuous phase always impacts the discrete phase, you can also incorporate the effect of the discrete phase trajectories on the continuum. This two-way coupling is accomplished by alternately solving the discrete and continuous phase equations until the solutions in both phases have stopped changing. The source term in the continuity conservation equation my be written as

$$S_{i'} = \frac{\Delta m_p \dot{m}_{p_o}}{m_{p_o}\, \mathrm{d}\forall}, \tag{12}$$

where Δm_p is change in the mass of the particle in the control volume in a $\mathrm{d}t$, $\dot{m}_{po}$ initial mass flow rate of the particle injection tracked and m_{po} the initial mass of the particle. The mass evaporated may be expressed by

$$\Delta m_p(\mathrm{d}\forall) = m_p(t) - m_p(t-\mathrm{d}t) = N_{i'} M_{i'} A_p\, \mathrm{d}t, \tag{13}$$

where $\mathrm{d}t=\mathrm{d}s/(u_p+v)$, and $\mathrm{d}s$ is the fraction of trajectory incide of each $\mathrm{d}\forall$ considered; $M_{i'}$ is the molecular weight of specie i', A_p the droplet area and $N_{i'}$ the molar flux of vapour:

$$N_{i'} = K_c\left(C_{i',s} - C_{i',\infty}\right), \tag{14}$$

where $C_{i',s}$ is the vapor concentration at the droplet surface and $C_{i',\infty}$ vapor concentration in the bulk gas:

$$C_{i',s} = \frac{P_{sat}(T_p)}{R(T_p)} \qquad C_{i',\infty} = \frac{P_\infty x_{i'}}{RT_\infty}\ . \tag{15}$$

where $x_{i'}$ is the mass fraction of the specie i'. The mass transfer coefficient K_c is obtained by a correlation of Nusselt number given by Ranz y Marshall (1952) (a) y (b)

$$K_c = \frac{\mathrm{Nu}\, D_{i',m}}{D_p} = \frac{\left(2 + 0{,}6 \cdot \mathrm{Re}^{1/2} \mathrm{S_c}^{1/3}\right) D_{i',m}}{D_p}, \tag{16}$$

The source terms of momentum equation, F_i,and energy equation are given by the expressions

$$F_i = \left(\frac{18\mu}{\rho_p D_p^2} \frac{C_D \mathrm{Re}}{\partial x_i} \left(v_i - u_{p_i}\right) + g_i \frac{\left(\rho_p - \rho\right)}{\rho_p} + \frac{\rho}{\rho_p} u_{p_i} \frac{\partial v_i}{\partial x_i} \right) \frac{\dot{m}_{p_o}\, \mathrm{d}t}{\mathrm{d}\forall} \tag{17}$$

$$S_h = \left[\frac{\overline{m}_p}{m_{p_o}} C_p \Delta T_p + \frac{\Delta m_p}{m_{p_o}} \left(-h_{f_g} + h_{pyrol} + \int_{T_{ref}}^{T_p} C_{p,i}\, \mathrm{d}T \right) \right] \frac{\dot{m}_{p_o}}{\mathrm{d}\forall}, \tag{18}$$

where D_p is the diameter of the droplet and $\dot{m}_{p_o}$ is the mass flow of particles contained in that differential of volume, $\overline{m}_p$ the average mass of the particle in the control volume d$\forall$, m_{p_o} the initial mass of the particle, C_p the heat capacity of the particle, ΔT_p the temperature change of the particle in the control volume in the d$\forall$, Δm_p the change in the mass of the particle in the control volume d $\forall$, h_{fg} the latent heat of volatiles evolved, h_{pyrol} the heat of pyrolysis as volatiles are evolved, $C_{p,i}$ the heat capacity of the volatiles evolved, T_p the temperature of the particle upon exit of the control volume d$\forall$ and T_{ref} the reference temperature for enthalpy.

This equations system has been solved numerically by a 2D model with a finite volumes code (Fluent). A sensibility study of the grid size was carried out, and the optimal one was formed by 24.208 cells. The discretization scheme of the numerical model was "Presto" and a first order upwind scheme was used for the convective terms. The coupling between momentum and continuity equation by means of pressure was solved by the "Simple" algorithm of Patankar (1980).

4. Numerical Results

Up-to-date work on the Hydrosolar Roof, described in the introduction, was to model the system experimental and numerically. The mathematical model described before was applied to a situation where geometric characteristics were based on a second generation real prototype. As boundary conditions, variables related to the air mass flow in the channel as: ambient temperature, ambient humidity, solar radiation and wind; and variables related to the sprayed water as water mass flow or drop size distribution among others were fixed. In this point, it is interesting to emphasize that the solar radiation was simulated with a temperature gap between channel plates and ambient conditions. With the objective of focusing the calculation effort on the evaporation zone, wind effect was substituted by a longitudinal depression in the channel outlet. The next figure shows boundary conditions used to calculate the Hydrosolar Roof performance.

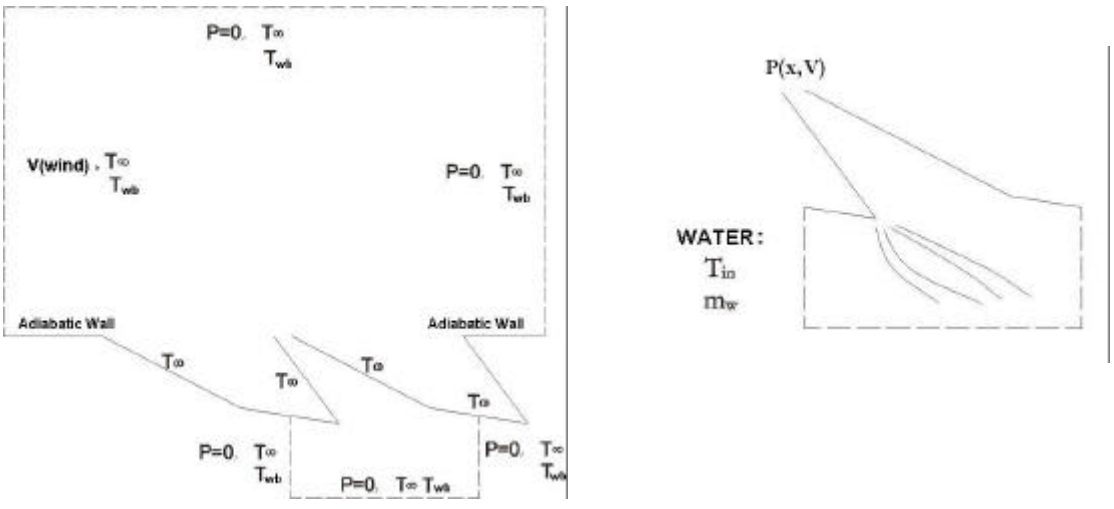

Figure 2: Boundary Conditions

Next table shows different parameters used to calculate, these were obtained from typical cooling tower design conditions described in Ashrae (1998)

PARAMETER	CASE
$T_{\infty}(\mathrm{K})$	300,15
$T_{wb}(\mathrm{K})$	298,15
$T_{in}(\mathrm{K})$	308,15
$\Delta T(\mathrm{K}) = T_{plates} - T_{\infty}(\mathrm{K})$	20
$V_w(\mathrm{m/s})$	1
$m_w(kg/s/m)$	0,0462

Table 1: Hydrosolar Roof performance calculation data

where T_{∞}(K) y T_{wb}(K) are dry and wet bulb ambient temperatures, T_{in}(K) is water inlet temperature, ΔT(K)=T_{plates}-T_{∞}(K) is temperature gap between plates and dry ambient temperature, V_w(m/s) is wind velocity and m_w(kg/s/m) is water mass flow per linear meter.

In Figure 3 it can be seen the streamlines in the starting case without interaction between the continuous and discrete phase. It can be observed that the air is ascending due to a natural and forced convection effect. Air rising through the channel is then used to exchange heat and mass with sprayed water from the bottom of the channel.

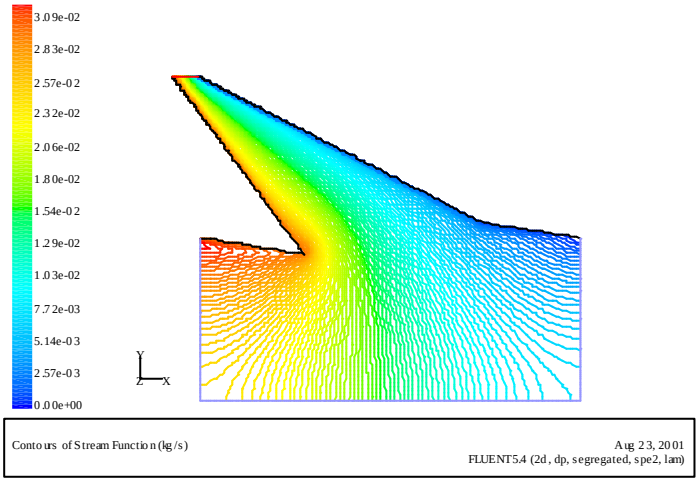

Figure 3: Air Streamlines

Next figures show temperature evolution in discrete phase and water mass fraction in continuous phase. Figure 4 shows the water temperature evolution from the inlet water temperature at the nozzle to the outlet water temperature on the floor of the building roof. Figure 5 shows the high water concentration in the continuous phase due to evaporation in the sprayed zone.

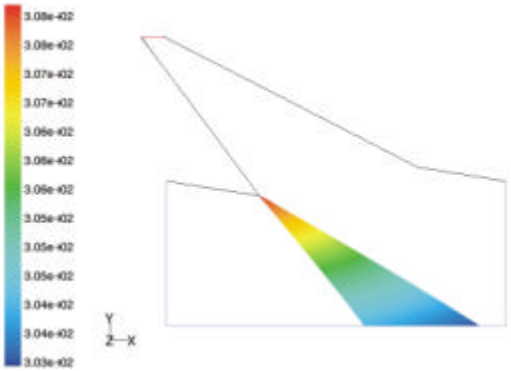

Figure 4: Water temperature evolution (K)

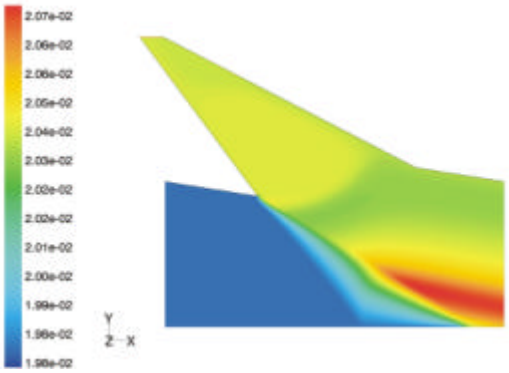

Figure 5: Water mass fraction (K)

A very important parameter in the evaporative cooling is the efficiency, defined as:

$$e = \frac{T_{in} - T_{out}}{T_{in} - T_{wb}} = \frac{\Delta T}{\Delta T_{\max}} \qquad (19)$$

where T_{out}(K) is water outlet temperature. Efficiency depends on thermodynamic and cooling tower geometric conditions. Present study is only interested in the influence on efficiency of one thermodynamic parameter (maximum water temperature difference by means of varying inlet water temperature and fixing ambient wet bulb temperature) and one geometric parameter (drop size). The rest of the parameters, that is, ambient conditions and water mass flow are constant. In order to validate the numerical procedure a comparison between numerical efficiency and maximum water temperature difference was carried out. This can be observed in Figure 6 where both numerical and experimental tendency are equals. This real comparison is obtained with a medium water drop size diameter of 600 μm, estimated from the catalogue information.

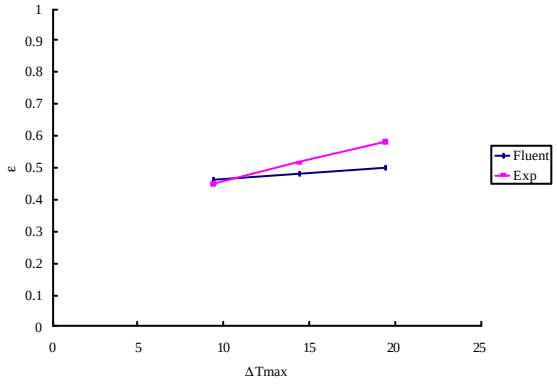

Figure 6: Experimental and Numerical Efficiency Comparison vs. DT_{max} (D_p = 600 mm)

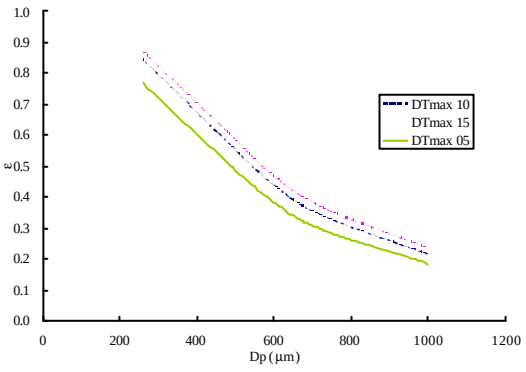

Figure 7: Numerical resultsy of Efficiency vs. D_p and DT_{max}

Figure 7 summarized all the calculated cases to obtain the influence of the drop size diameter and maximum water gap temperature on the efficiency. It can be observed that the smaller the drop size, the higher the efficiency. Nevertheless, to reduce the water droplet size only there has to be, to a selected nozzle,an increase in the pumping pressure. This is the link to the optimisation phase.

5. Optimization and discussion

The cornerstone of this section will be to decide which is the most suitable water drop size and, therefore, water pumping pressure. To achieve this objective, it has been necessary to include catalogue information and a vapor compression refrigeration cycle model.

As it can be observed in the previous section, to reduce drop size produces a higher efficiency. On the contrary, it is necessary to increase the pumping energy to reduce water drop size. The curve that relates pressure and water drop size is essential information for the optimization. To obtain this curve is necessary to define the nozzle size and kind. In the prototype built there were installed Flat Spray nozzles with an orifice size of 1 mm in diameter. Curve of pressure vs. drop size is obtained by adjusting data supplied by nozzles manufacturers.

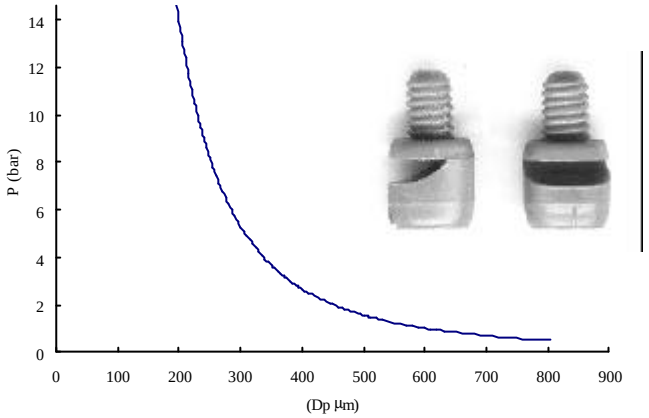

Figure 8: Pressure vs. drop size

To find the optimal pressure it is necessary to study the whole system, that is, not only the condenser as an isolated element, but also the others elements of the refrigeration cycle. Actual single-state vapor compression refrigeration cycle has been modelled with commercial software. This tool was useful to obtain a relation between energy consumed by the compressor and condenser temperaturem In this way it is possible to related the Hydrosolar Roof efficiency improvement with the others elements of a cooling system. With a chiller standard values using R-134a of useful overheating (4ºC) and useless overheating (3ºC) at the evaporator exit, pressure drops in suction line (9800 Pa) and discharge line (19600 Pa), underheating at condenser exit (2ºC) mechanical-electrical compressor efficiency (0.92) and isentropic compressor efficiency (0.9) and with a constant evaporator temperature (4.5 ºC) the following figure has been obtained:

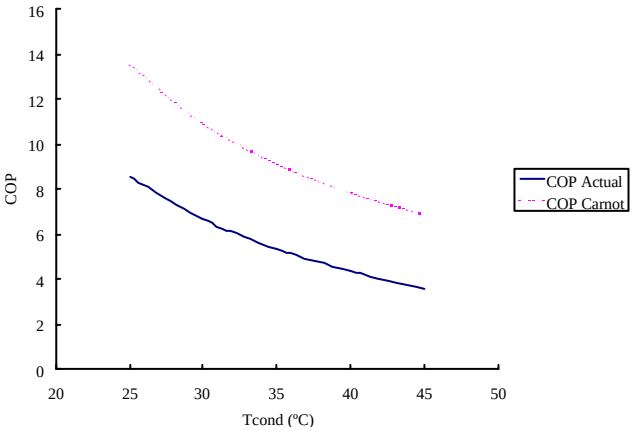

Figure 9: COP vs. condensation temperature

Then an integration of the results obtained with Fluent, data from catalogue and results from the refrigeration cycle was necessary. In this moment, the size of a prototype built at Technical University of Cartagena (Spain), 4x6 meters in length cell rows, was selected to develop the optimisation. The selected values are presented in the next table. With the inlet water conditions, that is, mass flow, temperature and drop size; and ambient conditions, efficiency is obtained. Water outlet temperature is deduced from the efficiency and, then, condensation temperature with a standard difference between refrigerant and water. With evaporation and condensation temperature it is possible to calculate the coefficient of performance (COP Cycle) and the energy exchange in the refrigeration cycle. After that, a global coefficient of performance (COP Global) is defined as the relation of absorbed energy from the cold region and the consumed energy by the compressor and the pump.

P (bar)	1	**T_{out} (ºC)**	30,55855075
D_p (mm)	600	**T_{cond} (ºC)**	37,77927537
m_w(Kg/s)	1,11	**T_{evap} (ºC)**	4,5
$W_{Pumping}$ (W)	112,36974	***COP (Cycle)***	4,720420544
Hydrosolar Roof Efficiency	0,444145	**Q_{cond} (W)**	20607,43624
T_{wb} (ºC)	25	**W_{comp} (W)**	3602,433787
T_{in} (ºC)	35	**Q_{evap} (W)**	17005,00246
DT_{max} (ºC)	10	**W_{total} (W)**	3714,803527
DT (ºC)	4,441449253	***COP (Global)***	4,577631719

Table 2: Performance Data

Starting from this data, different situations were studied maintaining the refrigeration capacity. The solution to these cases presents two clear tendencies, varying water drop size, showed in Figure 10 as the pressure is higher, obviously, the pumping pressure is higher too, but the power consumed by the chiller compressor is lower. That is in this way due to lower condensation temperature because of better condenser efficiency.

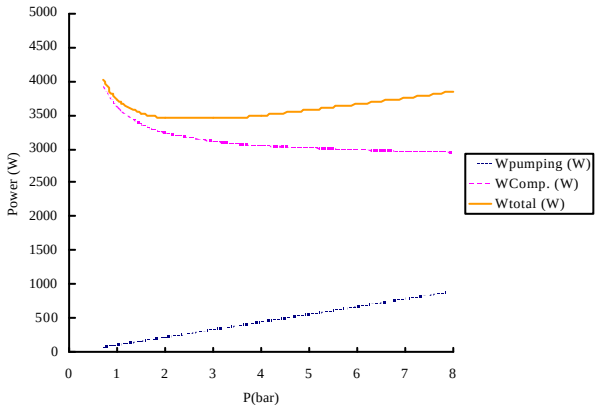

Figure 10: Power consumed vs. Pressure

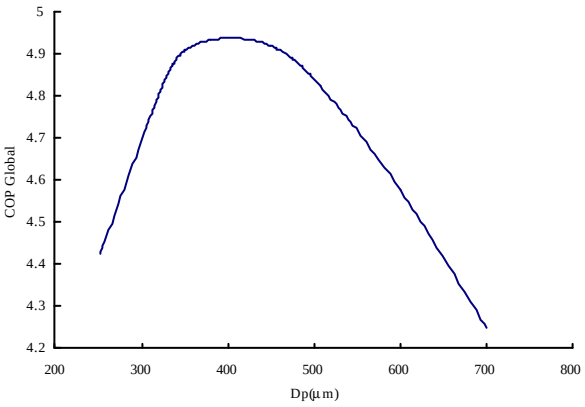

Figure 11: COP vs. Drop Size Diameter

Figure 11 shows the curve object of this paper, it can be seen that the optimum coefficient of performance is on a Drop size value of 400 µm, this value corresponds to a pumping pressure of 2.66 bar. With these modifications an energy savings of 7.5% has been obtained compared with the present operation point (1 bar).

6. Conclusions

Conclusions achieved in this study can be summarized as follows:

- Hydrosolar second generation Roof direct contact heat and mass transfer simulation have been developed with a CFD code.
- Numerical results have been compared with the experimental results obtained previously in Hydrosolar Roof prototype.
- Drop size optimization has been carried out and it has been necessary to include catalogue information and a vapor compression refrigeration cycle model.
- Optimum coefficient of performance with a Drop size value of 400 μm has been found.
- As future studies can be planned a 3D simulation or modification of with the water mass flow at the same time as modifing the drop size.

7. Acknowledgements

The authors wish to acknowledge the collaboration in the calculations of A. Navarro, as well as José María Galán, Energy, Comfort and Environment S.L. manager, as proposer of the original idea.

8. References

Merkel, F., 1925, Verdunstungskuehlung, VDI Forchungarbeiten No.275.

Nottage, H. B., 1941,Merkel´s cooling diagram as a performance correlation for air water evaporative cooling system, ASHVE Trans. 47, 429.

Mohiuddin, A. K. M., Kant, K., 1996, Knowledge base for the systematic design of wet cooling towers, I. J. Refrig, V. 19, No. 1, pp. 43-51.

Benton, D. J., Waldrop, W.R., 1988, Computer simulation of transport phenomena in evaporative cooling towers, I. J. H. T., V. 110, pp. 190-196.

Milosavljevic, N., Heikkila, P., 2001, A comprehensive approach to cooling tower design, Applied Thermal Engineering., V. 21, pp. 899-915.

Kaiser, A. S., Viedma, A., 2001, Hydrosolar roof for integrated energy dissipation and capture in buildings, Energy and Building, No.33, pp. 673-682.

Kaiser, A. S., Martínez, P., Lucas, M., Viedma, A., (a) 2001, Presentación del Prototipo de Techo Hídrico solar para la evacuación y captura de energía térmica en climatización de edificios, I Encuentro RIRAAS, Sevilla.

Zamora, B., Kaiser, A. S., Martínez, P., Lucas, M., 2000, Simulación numérica de la convección natural en una chimenea hídrico-solar, Fluent Users Meeting, Barcelona.

Kaiser, A S., Lucas, M., Zamora, B., (b) 2001, Estudio de extractores estáticos para la optimización del gasto en una chimenea hídrico-solar, Fluent Users Meeting, Madrid.

Kaiser, A S., Lucas, M., Martínez, P.,Viedma, A., Zamora, B., 2002, Simulación numérica de la transmisión de calor por evaporación producida en una torre de refrigeración extendida, CYTEF, Cartagena, Abril.

Morsi, S. A., Alexander, A. J., 1972, An Investigation of Particle Trajectories in Two-Phase Flow Systems. J. Fluid Mech., 55(2):193--208, September 26.

Ranz, W. E., Marshall, W. R., (a) 1952, Evaporation from Drops, Part I. Chem. Eng. Prog., 48(3):141--146, March.

Ranz, W. E., Marshall, W. R., (b) 1952, Evaporation from Drops, Part II. Chem. Eng. Prog., 48(4):173--180, April.

Patankar, S. V., (1980).Numerical Heat Transfer and Fluid Flow. Hemisphere, Washington.

Ashrae Handbook., 1996, HVAC System and Equipment, Chap. 36.